RESEARCH/REVIEW ARTICLE

Warming of Atlantic Water in two west Spitsbergen fjords over the last century (1912–2009)

Alexey K. Pavlov,[1] Vigdis Tverberg,[2,3] Boris V. Ivanov,[1,4] Frank Nilsen,[5,6] Stig Falk-Petersen[7,8,2] & Mats A. Granskog[2]

[1] Arctic and Antarctic Research Institute, RU-199397 St. Petersburg, Russia
[2] Norwegian Polar Institute, Fram Centre, NO-9296 Tromsø, Norway
[3] Faculty of Biosciences and Aquaculture, University of Nordland, NO-8049 Bodø, Norway
[4] Department of Oceanology, St. Petersburg State University, RU-198178 St. Petersburg, Russia
[5] Department of Arctic Geophysics, University Centre in Svalbard, NO-9171 Longyearbyen, Norway
[6] Geophysical Institute, University of Bergen, NO-5020 Bergen, Norway
[7] Akvaplan-niva, Fram Centre, NO-9296 Tromsø, Norway
[8] Faculty of Biosciences, Fisheries and Economics, University of Tromsø, NO-9037 Tromsø, Norway

Keywords
Temperature; West Spitsbergen Current; Atlantic Water; ERA reanalysis; warming; Svalbard.

Correspondence
Alexey K. Pavlov, Arctic and Antarctic Research Institute, 38 Bering St., RU-199397 St. Petersburg, Russia.
E-mail: pavlov.alexey.k@gmail.com

Abstract

The recently observed warming of west Spitsbergen fjords has led to anomalous sea-ice conditions and has implications for the marine ecosystem. We investigated long-term trends of maximum temperature of Atlantic Water (AW) in two west Spitsbergen fjords. The data set is composed of more than 400 oceanographic stations for Isfjorden and Grønfjorden (78.1°N), spanning from 1876 to 2009. Trends throughout the last century (1912–2009) indicate an increase of 1.9°C and 2.1°C in the maximum temperature during autumn for Isfjorden and Grønfjorden, respectively. A recent warming event in the beginning of the 21st century is found to be more than 1°C higher than the second warmest period in the time series. Mean sea-level pressure (MSLP) data from ERA-40 and ERA-Interim data sets produced by the European Centre for Medium-Range Weather Forecasts and mean temperature in the core of the West Spitsbergen Current (WSC) at the Sørkapp Section along 76.3°N were used to explain the variability of the maximum temperature. A correlation analysis confirmed previous findings, showing that variability in the oceanography of the fjords can be explained mainly by two external factors: AW temperature variability in the WSC and regional patterns of the wind stress field. To take both processes into consideration, a multiple regression model accounting for temperature in the WSC core and MSLP over the area was developed. The predicted time series shows a reasonable agreement with observed maxima temperature in Isfjorden for the period 1977–2009 ($N = 24$), with a statistically significant multiple correlation coefficient of 0.60 ($R^2 = 0.36$) at $P < 0.05$.

The general pattern of ocean circulation in the Greenland, Icelandic and Norwegian (Nordic) seas, as well as in the Fram Strait, has long been known (e.g., Coachman & Aagaard 1974). Atlantic Water (AW) is the dominant oceanic heat source to the Arctic Ocean (Nansen 1915; Ganachaud & Wunsch 2000; Rudels et al. 2000). AW originates from the Gulf Stream and continues on as the North Atlantic Current. Passing through the Faroe–Shetland Channel, it flows along the continental slope of Norway as the Norwegian Atlantic Current. North of Norway, it splits into two branches: the North Cape Current (Barents Sea Branch) flowing eastward into the Barents Sea and the West Spitsbergen Current (WSC) (Fram Strait Branch) that flows northward into the Fram Strait. Recent volume budgets studies have indicated that the WSC is estimated to transport the majority of the

Citation: *Polar Research* 2013, *32*, 11206, http://dx.doi.org/10.3402/polar.v32i0.11206

volume flux of AW (Schauer et al. 2008; Smedsrud et al. 2010) and is also responsible for the major heat transport towards the central Arctic (e.g., Aagaard & Greisman 1975; Walczowski et al. 2007).

As the only deep connection between the North Atlantic and the Arctic Ocean, the Fram Strait is the key region for water exchange and fluxes between the Arctic and sub-Arctic. In addition to the WSC, circulation in the Fram Strait consists of the East Greenland Current (EGC), carrying cold and relatively fresh Polar Water from the Arctic. It flows southward along the east Greenland continental slope. The EGC transports the major part of the drifting sea-ice from the Arctic Basin (Vinje 2001; Kwok 2009). In central Fram Strait, between the EGC and the WSC, there is a complex circulation pattern with high mesoscale activity and a recirculation (Johannessen et al. 1987).

The WSC not only plays a substantial role for the sub-Arctic–Arctic heat and volume exchanges but also is of utmost importance for regional Svalbard oceanography and marine biological communities. Due to conservation of potential vorticity, the WSC is strongly topographically steered along the steep continental slope, where the core with maximum temperature, salinity and current speed has been observed (Hanzlick 1983; Saloranta & Haugan 2004). Less saline and relatively cold Arctic-type Water (ArW) also flows northwards over the continental shelf, forming a barrier for west Spitsbergen fjords from a direct impact of warm AW. Usually, a strong front marking the boundary between these two types of water is observed in the area known as the Arctic Front (Saloranta & Svendsen 2001). Exchange across this front has been linked to northerly winds through surface offshore Ekman drift, resulting in upwelling in the WSC. The resultant altering of the horizontal density gradient is believed to trigger this exchange (Svendsen et al. 2002; Cottier et al. 2007). Detailed studies of the exchange process indicate that when conditions are favourable (often wind-induced), the front develops meanders and eddies due to either barotropic (from cross-frontal horizontal current shear) or baroclinic instability (from cross-frontal density gradient). Such meanders and eddies (stable and unstable shelf waves) have been detected in current meter time records in the WSC and found to account for heat flux towards the shelf and fjords (Nilsen et al. 2006; Teigen et al. 2010). Numerical modelling with a mesoscale eddy resolving grid also shows that eddies are responsible for flux of AW towards the fjords (Tverberg & Nøst 2009).

The balance of AW and ArW influx, river run-off and glacial melt dominates physical conditions in the west Spitsbergen fjords, and processes connected to sea-ice formation and melting (Cottier et al. 2005). Recently, anomalously warm water masses and reduced sea-ice formation has been observed (Zhuravskiy et al. 2012). These changes have had a profound impact on local marine ecosystem structure and functioning (e.g., Hop et al. 2002; Basedow et al. 2004; Berge et al. 2005; Berge et al. 2009). The connection with the Arctic Front exchange processes was clearly illustrated in one particular incident during which northerly winds led to AW penetrated over the continental shelf and into the fjords (Cottier et al. 2007). These warm and saline intrusions are most pronounced during summer and are believed to be an important mechanism for exchange of fjord waters (Ingvaldsen et al. 2001; Svendsen et al. 2002; Cottier et al. 2005; Cottier et al. 2007; Tverberg & Nøst 2009; Teigen et al 2010).

Saloranta & Haugan (2001) conducted an investigation of long-term variability of the WSC hydrography (Saloranta & Haugan 2001). However, the short time scales of atmospheric forcing events that result in the AW intrusions (Cottier et al. 2007) make it difficult to assess how conditions off the shelf represent the conditions inside fjords. An attempt was made to estimate the long-term variability of oceanographic conditions in one of the west Spitsbergen fjords (Kongsfjorden) by Tverberg et al. (2007), but the sparse data available did not allow for the resolution of trends in temperature and salinity before the 1970s.

A better understanding of the hydrography of the west Spitsbergen fjords through the past century would be valuable for accurate modelling of landfast ice in the fjords (Andreev & Ivanov 2001) and for ecosystem and biological studies (Berge et al. 2009). In this study, we examine the available historical data from west Spitsbergen fjords in order to construct longer time series and to consider the main trends and inter-annual variability of oceanographic properties over the last century. We aim to answer two questions: (1) how strong was a recent (beginning of 21st century) warming period in two west Spitsbergen fjords compared to conditions during 20th century?, and (2) what could be the dominant drivers of the observed variability of hydrography in the area under study?

Materials and methods

Study area

Several west Spitsbergen fjords were initially considered. Hornsund, Isfjorden and Kongsfjorden are traditionally among the most studied areas in the region, with the largest data sets available. Of the accessible data for Hornsund, the most reliable information comes from the month of July, which does not correspond to the period

Citation: *Polar Research* 2013, *32*, 11206, http://dx.doi.org/10.3402/polar.v32i0.11206

we eventually chose to consider, August–October (see below). Data from Kongsfjorden covers the last three decades (Tverberg et al. 2007); however, the data coverage is too poor to be included in the current study.

Two interconnected areas were chosen for this study: (1) the outer part of Isfjorden and (2) Grønfjorden (Fig. 1). The choice is based on the availability of historical data. With a location in the central part of west Spitsbergen, hydrographic processes in Isfjorden and Grønfjorden are similar to other large fjords, such as Kongsfjorden and Hornsund, and therefore key results obtained from this study could be regarded as a representative for other west Spitsbergen fjords.

Isfjorden is the largest of the west Spitsbergen fjords. The mouth of the fjord is connected to the adjacent continental shelf by a comparatively deep area with depths reaching 450 m. Because there is no topographic barrier between the outer fjord and the shelf, AW intrusions can freely propagate inwards through the Isfjorden mouth. Further east, at approximately 14°20′E, the bottom rises to depths of about 200 m (Fig. 1).

Grønfjorden is a comparatively small fjord, 16–18 km long and 2–5 km wide, adjacent to outer Isfjorden, where the settlement of Barentsburg is located. As for Isfjorden, the exchange of water masses is not restricted by a sill. The bathymetry of Grønfjorden is rather simple, spanning from 180 m at the entrance to 140 m in the central part (Fig. 1).

Regional settings

Since the primary objective of the study is to investigate AW in the fjords, we provide here a brief overview of

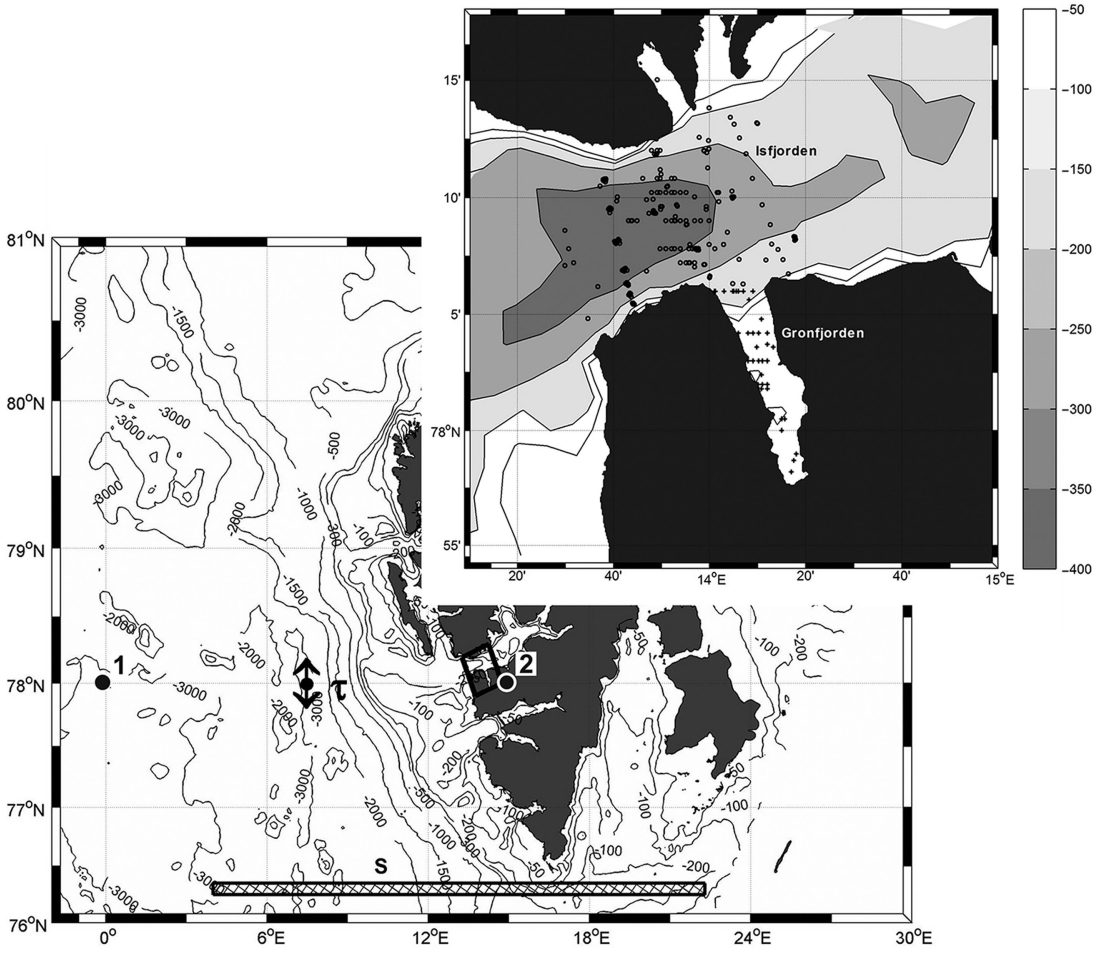

Fig. 1 Map of Svalbard and the eastern part of Fram Strait. Locations of the atmospheric forcing data points (1, 2 and τ), the Sørkapp Section along 76.3°N (S) and the study area (box) are depicted. The inset shows Grønfjorden and the outer part of Isfjorden. Positions of historical oceanographic stations are shown for Isfjorden (circles) and Grønfjorden (crosses). The colour bar reflects the bottom topography and is based on Jakobsson et al. (2008).

regional water mass classification. AW, coming directly from the WSC is defined as waters warmer than 3°C with salinity greater than 34.9 (Swift & Aagaard 1981). Transformed AW with a temperature between 1°C and 3°C, and salinity ranging from 34.7 to 34.9, is the product of mixing between AW and ArW on the shelf, and it is the most common water mass for west Spitsbergen fjords (Svendsen et al. 2002; Cottier et al. 2005; Nilsen et al. 2008). Surface Water is typically found in a surface layer throughout spring, summer and early autumn. It is formed by the river run-off and glacial and sea-ice melt, and its salinity is lower than 34; its temperature is above 1°C, sometimes as high as 6°C −7°C in mid-summer (Cottier et al. 2005; Nilsen et al. 2008). Characteristics and sources of other water masses that we do not refer to in this article (Winter Cooled Water, Local Water and Intermediate Water) are not described here. Detailed overviews of specific water masses can be found in Svendsen et al. (2002) and Nilsen et al. (2008).

Oceanographic data set

Oceanographic observations in west Spitsbergen waters started at the end of the 19th century and have continued until today, with a shift from sampling with Nansen bottles to modern conductivity–temperature–density (CTD) profiling in the late 1970s. In this study, we use several different data sources. The major sources are the International Council for the Exploration of the Sea (ICES) oceanographic database and data collected by the World Data Centre (WDC), Obninsk, Russia, containing some older data coming from Russian fisheries. These data sets were complemented by more recent data collected by the Norwegian Polar Institute (NPI); the Arctic and Antarctic Research Institute (AARI), St. Petersburg; and the University Centre in Svalbard (UNIS). In total, the assembled oceanographic data set comprises 415 oceanographic stations covering the period from 1876 to 2009. The temporal distribution of data is inhomogeneous from year to year and covers the months from April to December.

A data set from the core of the WSC, assembled by the Institute of Marine Research (IMR), in Norway, was also considered. These data consist of mean temperature and salinity in the core of AW (50–200 m) observed every autumn between August and October (Lind & Ingvaldsen 2012) at the Sørkapp Section, running westwards from the southern tip of Spitsbergen along 76°20′ N (Fig. 1). The temporal coverage is from 1977 to 2009, with a one-year gap in 2003. For the joint analysis, we use only temperature data (denoted hereafter as T_{WSC}).

Selection of data: spatial, temporal and vertical. Although the WDC and ICES data sets are claimed to be quality checked, we carried out some basic checks to detect any obvious errors and spikes. Because around 35% of the stations' salinity data is missing, we omitted the salinity time series and focussed only on temperature in this study. With the exception of the uppermost layer, which is excluded from the analysis, water temperature is a reliable proxy for tracing AW within such a naturally cold environment as the west Spitsbergen fjords (e.g., Cottier et al. 2005).

To demonstrate this, temperature and salinity profiles taken from CTD stations in Isfjorden are plotted (fall data, 2007–09). We use the graph presented in Fig. 2 to select the typical depth range at which temperature alone could be used as a good indicator of AW presence. The surface layer is influenced by river run-off and glacial melt, transporting loads of suspended particulate matter, which contribute to stronger solar heating throughout summer and the beginning of autumn. In Fig. 2, the low salinity waters were found down to 75–100 m and the isohaline 34.7 (Svendsen et al. 2002) can be used to distinguish between water masses of Atlantic, Arctic and local origin. A similar plot for Grønfjorden (not shown) demonstrates the influence of surface waters down to 50–75 m. Therefore, in this study, we exclude a surface layer of

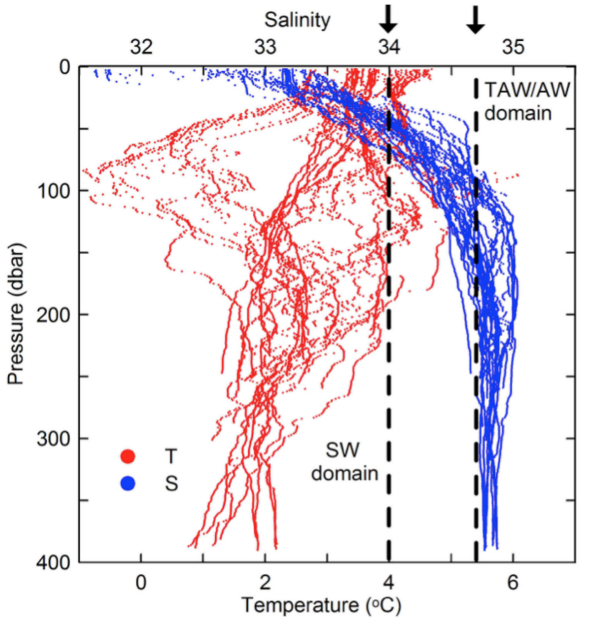

Fig. 2 Temperature and salinity profiles for the Isfjorden domain, autumn 2007–09. Salinity of 34.0 and 34.7 are depicted by black dashed lines. Surface Water (SW), Transformed Atlantic Water (TAW) and Atlantic Water (AW) are indicated.

Citation: *Polar Research* 2013, *32*, 11206, http://dx.doi.org/10.3402/polar.v32i0.11206

75 m for Isfjorden and of 50 m for Grønfjorden from further analysis.

Studies in Kongsfjorden and Isfjorden (Cottier et al. 2005; Nilsen et al. 2008) indicate that, in general, west Spitsbergen fjords can be characterized as having a bimodal distribution of oceanographic conditions: AW dominates in late summer, and cold, locally produced water masses and ArW dominate in winter. Although AW inflow has recently been observed also in the winter (Cottier et al. 2007), the most likely time to find AW in the fjords is in summer. To account for the time needed to replace the locally produced water mass with the new AW, the early summer season observations should be excluded from analysis.

For our study, we use only autumn data collected from August to October, assuming that there is the highest probability that, by the beginning of August, oceanographic conditions become AW-dominated and that, before the end of October, cooling and subsequent ice formation and winter convection do not affect water of Atlantic origin inside the fjords. These two assumptions are generally realistic and are confirmed by field observations (Svendsen et al. 2002; Cottier et al. 2005; Nilsen et al. 2008). Also, the selected months contain a major fraction of the observations. Of all the available data from June to November, 72% of the stations are from August to November, with a slight increase in sampling during these months in the era of CTD observations.

The choice between average and maximum temperatures. The initial idea of this work was an investigation of long-term variability of average and maximum/anomalous AW temperatures in Isfjorden and Grønfjorden. The major challenge, which was encountered during the analysis of average conditions, is the spatial heterogeneity of AW at the mouth of Isfjorden. Cross-fjord sections (not presented here) show significant lateral differences in temperature, similar to those described by Nilsen et al. (2008: 1843, figure 5). The width of Isfjorden is approximately twice the local internal Rossby radius of deformation (Svendsen et al. 2002; Nilsen et al. 2008), so Coriolis effects on the circulation cannot be neglected. AW enters the Isfjorden system along the southern coast and the difference in temperature can exceed 1°C –2°C at the same depth in different parts of cross-fjord transect. One way to account for these uncertainties is to divide the Isfjorden mouth into two or more domains with similar properties, but due to data limitations the new data sets would become sparser and less suited to statistical analysis.

We therefore focus on the analysis of extreme oceanographic conditions with regard to the presence of AW. Using the maximum temperature is based on the thorough analysis of the obtained data set and is similar to approaches in previous studies of AW propagation into the Arctic Ocean (e.g., Trešnikov & Baranov 1972; Treshnikov 1977; Carmack et al. 1995).

Simultaneous use of bottle and CTD data. When working with historical data sets, it can be a challenge to combine historic data collected with Nansen bottles at standard depths and modern high-resolution continuous profiles obtained by CTD profilers after the late 1970s. For some goals, bottle data can be interpolated onto a grid with a finer resolution (e.g., Saloranta & Haugan 2004). In our particular case, CTD profiles (Fig. 2) show the presence of fine structure and frequent alternation of temperature and salinity with depth. Taking this into consideration, along with the fact that most of the data used here comes from Nansen bottles, we decided not to add additional errors and uncertainties by making any interpolations of bottle data.

Instead, all CTD profiles were processed such that values at "fixed" standard depths were extracted. For the analysis of maximum temperatures in the AW layer, this procedure leads to an incorrect description of temperature maxima in the profile. Peaks of temperature could fall in between standard depths and, as a consequence, will be lost and substituted by colder values. This leads to a systematic underestimation of maximum temperatures in each profile.

Following Grotefendt et al. (1998), who investigated uncertainties of Russian climatological data in the Arctic, we performed a comparative study of the potential effect of the technique mentioned above on further data analysis. To do that, we selected all CTD profiles for Isfjorden ($N = 168$) and Grønfjorden ($N = 18$) and constructed our "fixed bottle" profiles. CTD profiles were sub-sampled at the standard depths of bottle data (0, 25, 50, 75, 100, 125, 150, 200, 250, 300, 350, 400 m and bottom) and the difference between maximum temperature from each full and sub-sampled CTD profile was calculated.

The maximum error originating from coarser bottle data is 0.54°C for Isfjorden and 0.33°C for Grønfjorden, with mean differences of 0.075 ± 0.074 and 0.036 ± 0.053°C, respectively. Graphical results are presented in Fig. 3. To put these values in context, the year-to-year temperature difference of the constructed time series was calculated for consecutive years. The mean absolute difference was found to be 0.68 ± 0.66°C, which is one

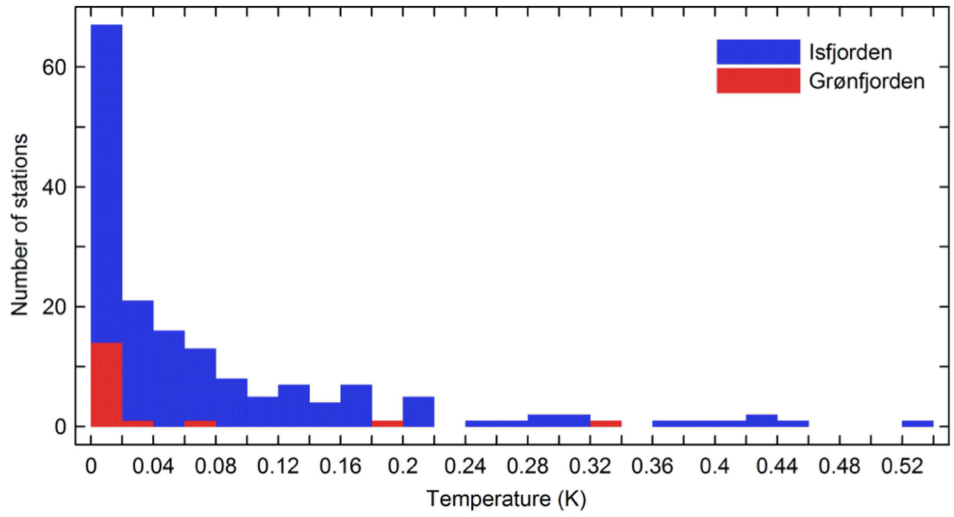

Fig. 3 Frequency histogram of differences between maximum temperatures of the profiles derived from conductivity–temperature–density sensors and Nansen bottles data.

order of magnitude higher than the mean differences in maximum temperature between CTD and bottle profiles, showing that deviations between the two maximum temperatures (CTD minus bottle) for each profile are relatively small. We believe that differences caused by the selection of "fixed" standard depths from CTD data do not result in significant errors into the joint analysis of CTD and bottle data. Subsequently, all late summer and autumn temperature profiles (August–October) were binned annually and within each bin a maximum AW temperature was found for further analysis.

ERA reanalysis data on Mean sea-level pressure

It has been shown, based on modelling and field observations, that intrusions of AW from the WSC onto the shelf and towards the fjords are correlated with strong northerly winds to the west of Svalbard (Svendsen et al. 2002; Cottier et al. 2007). Following geostrophic wind theory (e.g., Gill 1982), we expect the difference in MSLP along 78°N to be a reliable proxy for the meridional wind component over the WSC; therefore, we use supplementary meteorological data on MSLP in order to interpret and explain observed variability in our constructed time series of AW maximum temperature in the fjords.

We have chosen the products ERA-40 and ERA-Interim, produced by the European Centre for Medium-Range Weather Forecasts. The ERA reanalysis is recognized to be a reliable data set (e.g., Bromwich et al. 2007; Dee et al. 2011). Recently, the ERA-40 reanalysis was supplemented by a product known as ERA-Interim. Both consist of a comprehensive set of global meteorological analyses, covering the periods 1957–2002 (ERA-40) and 1989–present (ERA-Interim). Intercomparisons between ERA-40 and ERA-Interim data sets have not been done previously for the Fram Strait region.

Although it is not the main task of this particular study, we performed a basic statistical analysis of differences in MSLP in the ERA-40 and ERA-Interim data sets for our region. For that, we extracted data for the following domain: 15°W to 22.5°E, and 75°N to 82.5°N, covering the Fram Strait and adjacent parts of Svalbard. Since ERA-40 and ERA-Interim have different grid resolutions ($2.5^\circ \times 2.5^\circ$ for ERA-40 and $1.5^\circ \times 1.5^\circ$ for ERA-Interim), we selected those grid points within the selected domain that have the same coordinates. In total, 12 points were selected and an intercomparison (analysis of differences between the ERA-40 and ERA-Interim) using the 13 overlapping years (164 months) was performed for the monthly mean MSLP (Fig. 4).

The MSLP differences between the ERA-Interim and the ERA-40 time series ranges between -1.31 and 1.82 hPa. An average bias (ERA-40 and ERA-Interim) is 0.05 ± 0.26 hPa. The trend in differences over the intercomparison period (13 years) is ca. 0.001 hPa per month, which is negligible compared to absolute values of MSLP (mean of 1010.4 hPa for both reanalyses) over the considered period.

We consider the difference between ERA-Interim and ERA-40 reanalysis time series to be satisfactory for the goals of the present study. In addition, in the analysis, MSLP time series is used in terms of the difference between two grid points (see below), not as absolute values. This further reduces biases.

Citation: *Polar Research* 2013, *32*, 11206, http://dx.doi.org/10.3402/polar.v32i0.11206

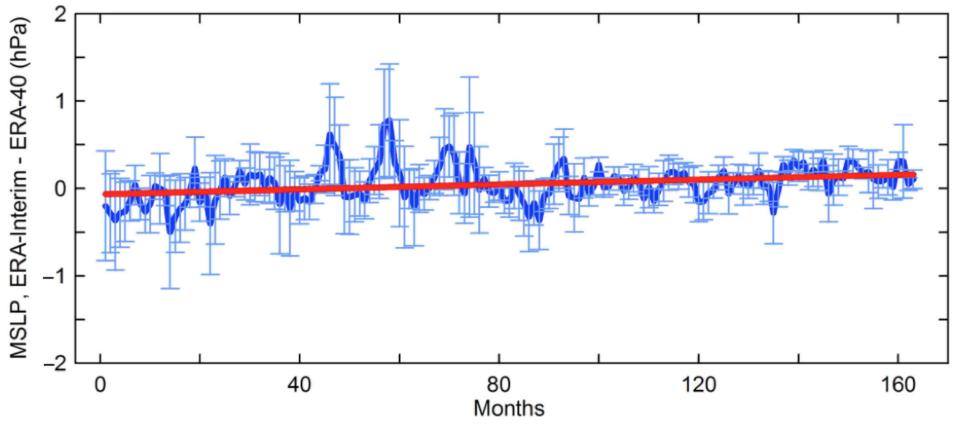

Fig. 4 The distribution of differences between monthly means of mean sea-level pressure (MSLP) (ERA-Interim and ERA-40 data sets) for each pair of coincident grid points of the selected domain ($N = 12$). The ensemble mean (thick line), a corresponding linear trend (slope = 0.001 hPa/month) and error bars denote the plus/minus one standard deviation of the mean. In total, 164 months are compared. The first month corresponds to September 1989, while month number 164 corresponds to August 2002.

For further analysis, we selected two points for MSLP: 0°E/W and 15°E along 78°N (Points 1 and 2; see Fig. 1), assuming that the difference in MSLP between these locations is representative of the meridional wind component at point 7.5°E and 78°N (Point τ; Fig. 1) in the proximity of the WSC core. Because a pressure field is generally more robust than a wind field, the former is used in this study. Additional analysis showed a strong correlation between difference in MSLP and meridional wind component ($R = -0.94$, $P < 0.05$). As the standard grid in ERA-40 reanalyses does not include 78°N, a linear interpolation was applied between the closest grid points, 77.5°N and 80°N, to get the time series used here. The two reanalysis data sets were combined using the ERA-Interim time series for the overlapping period.

Results

After sub-sampling the available data set in space and time (see above), 145 oceanographic stations for Grønfjorden and 270 oceanographic stations for Isfjorden were selected (Fig. 1), spanning from 1899 to 2009 and from 1876 to 2009, respectively. Because prior to 1912 only a few stations were available for both sites, only data after 1912 are used for the analysis, providing a time series of almost 100 years. The frequency distribution of stations is shown in Fig. 5a. Three distinct peaks in data availability can be seen: after 2002, the mid- and late 1980s (mostly in Grønfjorden) and the mid-1920s, associated with increased activities as the Russian settlement of Barentsburg was established.

Time series of maximum temperature measured in each year was constructed using data from 53 sampled years for Isfjorden and 27 sampled years for Grønfjorden (Fig. 5b). Visual analysis of the curves (Fig. 5b) indicates that maximum temperatures have always been above 0°C since 1912, suggesting that both fjords have been influenced by waters of Atlantic origin to a certain degree throughout the study period.

Both time series of maximum temperature are characterized by variations on different timescales: from decadal to interannual. Comparatively cold periods occur in 1912 in both fjords, in the early 1920s, early 1960s and late 1970s in Isfjorden, and in the 1990s in both fjords. Warm periods occur in the mid-1920s for both sites, in the mid-1930s in Grønfjorden, at the beginning and end of the 1960s and in the early 1970s in Isfjorden, and in the 1980s and after 2002 in both Isfjorden and Grønfjorden.

From Fig. 5b, it can be seen that an extremely strong warming event in comparison with earlier in the time series, occurred in the mid-2000s. For Isfjorden, maximum temperatures higher than 6°C were observed in 2006, which is more than 1°C warmer than the second warmest peak, in the 1980s. These results are consistent with the reported warming of WSC in this latest period (Walczowski & Piechura 2007; Schauer et al. 2008) and with recent palaeoceanographic findings from the WSC area (Spielhagen et al. 2011). A similar pattern, but with lower magnitude, is seen for Grønfjorden.

Figure 5c presents time series of maximum temperature in Isfjorden at all depths (75 m - bottom), and separately for the upper 75–200 m and 200 m - bottom. Subdivision at 200 m was done in order to distinguish between contributions of relatively mobile subsurface waters (shallower than 200 m) that could propagate into the mouth of Isfjorden from the shelf with similar depths, and deeper waters that could reside within the deep part of the

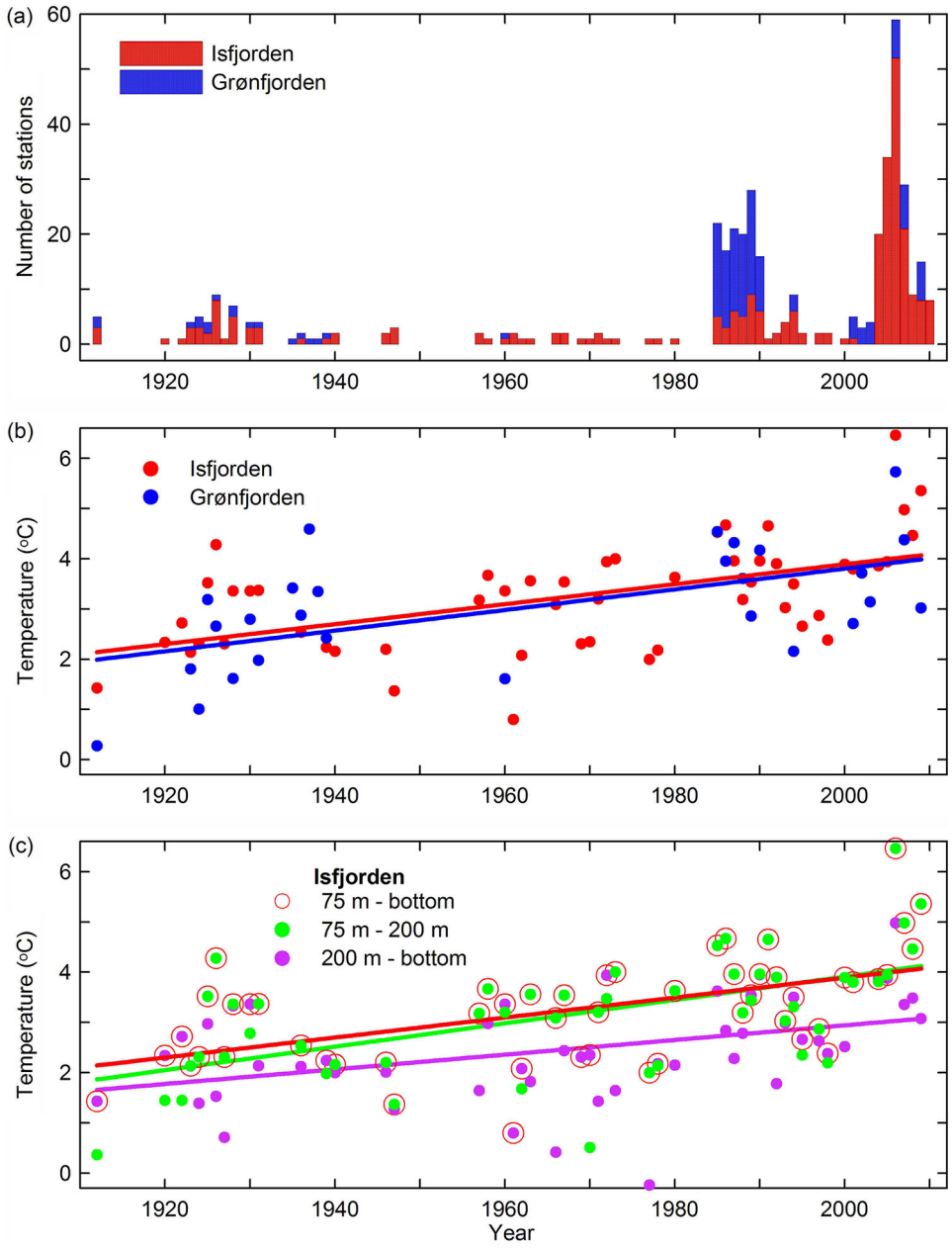

Fig. 5 (a) The availability of oceanographic stations; (b) time series of maximum Atlantic Water (AW) temperature at both locations with best-fit linear trend for the period 1912–2009; (c) time series of maximum AW temperature in Isfjorden for all depths (red), 75–200 m (green) and below 200 m (magenta) with best-fit linear trend for the period 1912–2009.

Isfjorden mouth longer. Throughout the time series, water with positive temperature was always present in both the upper and lower layers, except for 1977, when the maximum temperature below 200 m was below 0°C. Maximum temperatures for the upper 200 m were generally higher than those in the deeper layer.

In general, there is a gradual warming tendency in both Isfjorden and Grønfjorden. Linear trends ($T_{MAX} = A \times \text{Year} + B$) were estimated, as shown in Fig. 5b. Table 1 shows a summary of the linear regression and temperature trends. Despite the sparseness of the data sets, trends are very similar: ca. 0.19°C/decade for Isfjorden and ca. 0.21°C/decade for Grønfjorden. Both trends describe 28%–33% of existing variance ($R^2 = 0.28$ for Isfjorden and $R^2 = 0.33$ for Grønfjorden). The coefficients of determination for the trends are comparatively low

Citation: *Polar Research* 2013, *32*, 11206, http://dx.doi.org/10.3402/polar.v32i0.11206

Table 1 Summary for a linear regression. Temperature trends for Grønfjorden and for Isfjorden in various depth intervals during the period 1912–2009. Trends (*A* coefficients) are significant at $P < 0.05$.

Area		Years	*N*	*A*	*B*	R^2
Grønfjorden		1912–2009	27	0.021	−37.311	0.33
	75 m–bottom	1912–2009	53	0.019	−34.298	0.28
Isfjorden	75 m–200 m	1912–2009	51	0.023	−42.618	0.34
	200 m–bottom	1912–2009	51	0.015	−26.261	0.18

(Table 1), owing mostly to large variability within the time series that is not described by linear approximation. However, since both trends are statistically significant at $P < 0.05$ and the trend values are almost equal, the results are statistically reliable and are reasonable estimates.

The trends were found to be different for the different depth intervals in Isfjorden. The trend of maximum temperature below 200 m (ca. 0.15°C/decade) is lower in comparison with overall trends, while the trend for depths above 200 m (ca. 0.23°C/decade) is the highest among them. This highlights the relevance of the observed overall warming as it is most pronounced in the upper 200 m (excluding the uppermost 75 m).

Discussion

The revealed pattern of variability in the time series of maximum temperature (Fig. 5b) is similar to the findings of Polyakov et al. (2004), who investigated a long-term variability of Intermediate AW in the Arctic Basin based on similar historical data sets. The difference can be attributed to the time needed for the AW signal to propagate from the WSC area towards the central Arctic Basin. It has been recently shown that this time could vary significantly between years, with some average estimates of 2–5 years for the Laptev Sea and up to a decade for the Canadian Basin (Polyakov et al. 2011). For example, a warming period throughout the late 1920s and 1930s in the records from the Arctic Ocean could be distinguished in the time series from both Isfjorden and Grønfjorden, where it was observed several years earlier—around 1925. Some warm and cool periods are also in agreement with the study by Carton et al. (2011) of interannual variability of AW in the Nordic seas during 1950–2009. For example, a major cooling event at the end of the 1970s and a major warming in the mid-2000s in the Nordic seas are also pronounced in the time series of maximum temperature in Isfjorden and Grønfjorden.

During several periods in the time series—1912 to 1922, the 1970s and the end of the 1990s—warmer water was found in the deep layer, suggesting that warm waters could be found at the entrance of Isfjorden, even if no major intrusions of AW took place that particular year. This might be due to the residence of waters of Atlantic origin from the previous season, or to weaker intrusions of AW below the lighter Transformed AW or Local Water earlier in the summer, or both (Nilsen et al. 2008; Tverberg & Nøst 2009).

In addition, trends in maximum temperature for the sub-surface and bottom layers were found to be different (Fig. 5c, Table 1). One possible explanation for an enhanced warming in the upper layer might link it to changes in atmospheric circulation. Another mechanism might relate to a stronger eddy overturning on the shelf, but this is mostly pronounced in late winter and early spring (Tverberg & Nøst 2009).

In this work, we propose a simplistic statistical approach where we try to explain the observed variability in maximum temperature in Isfjorden based on additional data on temperature of the core of the WSC and atmospheric forcing over the WSC. The hypothesis to be tested is that on decadal time-scales, there is a statistical relationship between the observed temperature at the entrance of Isfjorden and the joint contribution of the temperature within the WSC as the source of the AW in the area and along-shelf winds over the WSC that could enhance the exchange between the WSC and the adjacent shelf (Cottier et al. 2007). Based on availability of data, we chose a period from 1977 to 2009 and focussed on Isfjorden only, where the time series is more complete than for Grønfjorden.

As supplementary information, we used data of monthly means of MSLP from the ERA-40 and ERA-Interim reanalysis. Different combinations were considered, such as monthly mean MSLP differences between various grid points to the west of Spitsbergen and differences averaged over several summer and autumn months. Among these options, an average MSLP difference between 0°E/W and 15°E along latitude 78°N for three autumn months (August–October) was found to give the best correlation with the observed temperature time series in Isfjorden. This dMSLP78 time series, as we refer to it hereafter, covers the period 1977–2009.

A comparison of time series of maximum temperature for Isfjorden, mean temperature in the core of the WSC along the Sørkapp Section (76.3°N) and dMSLP78 for the period 1977–2009 is shown in Fig. 6. In general, a

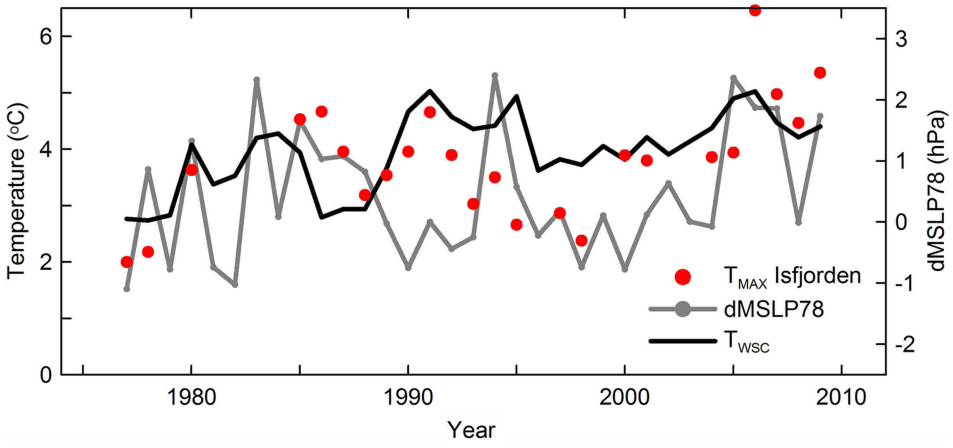

Fig. 6 Comparison of time series of maximum temperature for T_{MAX} Isfjorden, mean temperature in the core of the West Spitsbergern Current at the Sørkapp Section (76.3 N) T_{WSC} and dMSLP78 for the period 1977–2009.

similarity between maximum temperature for Isfjorden and the two other variables can be seen. The correlation coefficient R between T_{MAX} Isfjorden and dMSLP78 is 0.45, and the correlation coefficient between T_{MAX} Isfjorden and T_{WSC} is 0.46. Both coefficients are significant at $P<0.05$.

In order to consider the combined effect of mean temperature of the WSC upstream from the area under study and wind stress field (dMSLP78), a multiple regression equation has been introduced:

$$T_{MAX}\ Isfjorden = A \times T_{WSC} + B \times dMSLP78 + C, \quad (1)$$

where A and B are regression coefficients, and C is the intercept.

A comparison between the observed and predicted maximum AW time series for the period 1977–2009 is shown in Fig. 7, and the statistics are summarized in Table 2. The overall agreement between the observed and predicted curves is good (Fig. 7), with the proposed statistical model describing the main pattern of variability and a multiple correlation coefficient, $R=0.60$ ($R^2=0.36$). However, the model does not reproduce the cold period in the mid-1990s, and underestimates the amplitudes of warm peaks, for example, in the early 1990s and 2006 in Isfjorden, which might have originated from processes unaccounted for in the model. Both regression coefficients (A and B) are statistically significant at $P<0.05$. To assess which of the two variables has the greater effect in determining the value of maximum temperature in Isfjorden, beta weight coefficients (β_A and β_B) were estimated (Table 2). β_A and β_B represent the standardized coefficients of the unit-weighted regression equation, where the variables are standardized to have unit variances. Beta coefficients refer to the expected change in the dependent variable per standard deviation increase in each independent variable (e.g., Schroeder et al. 1986). Analysis shows that values of β_A and β_B are very close, with a slightly greater contribution from the mean difference in sea-level pressure (β_B). In addition, the same model was applied to the sub-divided (above and below 200 m) time series. For depth range 75–200 m, only β_B, representing the influence of atmospheric forcing, is statistically significant. In turn, below 200 m only β_A, accounting for the mean T within the WSC core is significant at $P<0.05$ (Table 2).

Results in this study contribute to the discussion over last decade about the potential mechanisms responsible for shelf–fjord water mass exchange. While several studies (Saloranta & Svendsen 2001; Cottier et al. 2007) have suggested that wind forcing induces barotropic instabilities and coastal upwelling, others focused on baroclinic instability at the Arctic Front as an important contributor to shelfward heat flux and AW intrusions towards the west Spitsbergen fjords (Tverberg & Nøst 2009; Teigen et al. 2011). Still, the knowledge about the mechanisms leading to frontal instabilities and processes responsible for eddy generation is not complete.

In our study, following Cottier et al. (2007), we focus our hypothesis on the substantial role of wind effects in the shelf–fjord water exchange. As found from model estimations, there is a statistically significant link between autumn maximum temperature in Isfjorden and a combined effect of temperature in the WSC and wind forcing, which confirms our initially posed hypothesis. Results for different depth intervals are of interest for linking with previous studies on wind-driven shelf–fjord exchange. We found that the wind effect is more pronounced for the subsurface layer. In our MSLP time series, we see that, during autumn, northerly winds are most common over the WSC (positive dMSLP78 values

Citation: *Polar Research* 2013, *32*, 11206, http://dx.doi.org/10.3402/polar.v32i0.11206

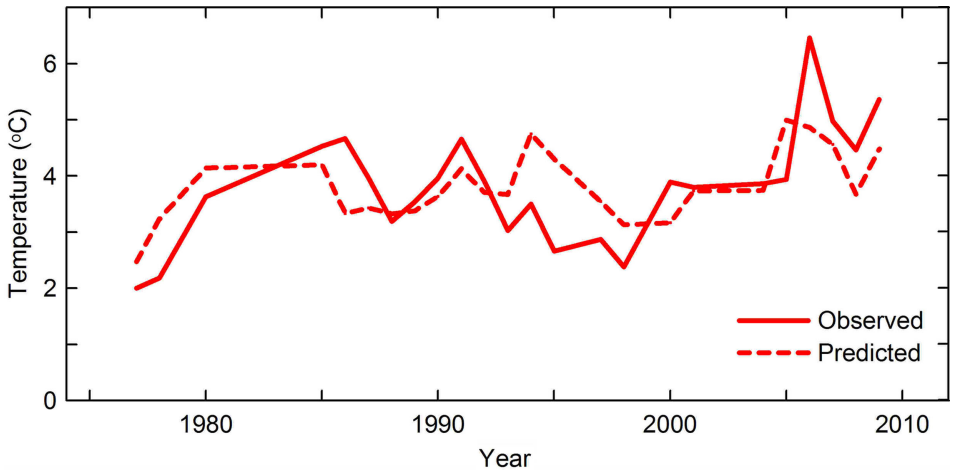

Fig. 7 Comparison of observed time series of maximum temperature for Isfjorden and predicted values based on a combination of mean temperature in the core of the West Spitsbergen Current at the Sørkapp Section and dMSLP78 for the period 1977–2009.

in Fig. 6). One could expect that northerly along-shelf winds would contribute to a shelfward AW inflow in a deeper layer (Klinck et al. 1981), demonstrating a significant positive relationship in the regression model for the deeper layer. However, our model results do not support this expectation. On the other hand, if the shelfward AW inflow occurs mainly at intermediate water depth, a wind induced stronger inflow of AW to the fjords would be more noticeable above rather than below 200 m in the water column. An intermediate depth inflow was modelled in a typical summer shelf edge front situation in Tverberg & Nøst (2009). At this point, it might be difficult to explain results based on simple phenomenological considerations.

Potential uncertainties could arise from not accounting for the pressure differences between the AW core in the WSC and the ArW (shelf water in the terminology of Tverberg & Nøst [2009]). Eddy exchange due to baroclinic instabilities is related to this cross frontal pressure gradient. An altered state of either AW or ArW could change the pressure gradient. It may be worthwhile to consider if the preceding winter ice conditions on the west Spitsbergen shelf can act as a preconditioning factor for the state of ArW in the summer. For example, the warm peak in 2006 coincided with the initiation of several years with no drift ice on the shelf, while the cold period in the mid- and late 1990s coincided with heavy ice conditions.

For future studies, to improve the performance of the suggested regression model and to better understand the processes of shelf–fjord exchange, the addition of sea-ice conditions (extent or concentration) and water properties across the Arctic Front would be in order.

Summary

Based on available data sets, long-term trends were estimated for autumn (August–October) maximum temperatures in the AW layer in Isfjorden and Grønfjorden (Spitsbergen). Trends for both Isfjorden and Grønfjorden are statistically significant and almost equal (ca. 0.19°C/ decade for Isfjorden and ca. 0.21°C/ decade for Grønfjorden), with an overall warming of 1.9°C and 2.1°C, respectively, for the period 1912–2009. The early-21st century warming event in west Spitsbergen fjords is substantially stronger (>1°C) in comparison with historical data throughout the 20th century. This is consistent with the reports of intensification and warming of the WSC core in the mid-2000s (Walczowski & Piechura 2007; Schauer et al. 2008) as well as with recent palaeoceanographic multidecade-scale studies over the past 2000 years to the west of Svalbard (Spielhagen et al. 2011).

Table 2 Summary for multiple regression analysis linking maximum temperature in Isfjorden in various depth intervals with two external predictors during the period 1977–2009. The predictors are the mean temperature in the core of the West Spitsbergen Current at 76.3°N (index A) and the difference in mean sea-level pressure along 78°N to the west of Svalbard (index B). β_A and β_B are standardized coefficients. Coefficients in parentheses are significant at $P < 0.05$.

Depths	*N*	β_A	*A*	β_B	*B*	*C*	*R*	R^2
75 m–bottom	24	(0.384)	(0.397)	(0.401)	(0.538)	1.413	0.603	0.363
75 m–200 m	24	0.359	0.519	(0.389)	(0.398)	1.449	0.575	0.330
200 m–bottom	22	(0.513)	(0.716)	0.344	0.328	−0.134	0.681	0.463

A simple model, developed on the basis of mean temperature of the WSC core at the Sørkapp Section (76.3°N) and the difference in MSLP (August–October) between 0°E/W and 15°E along 78°N, aids interpretation of the observed variation to a certain degree, with $R^2 = 0.36$; considering the variables separately (T_{MAX} Isfjorden vs. T_{WSC}, and T_{MAX} Isfjorden vs. dMSLP78) gives a corresponding R^2 of 0.21 and 0.22. Thus, it has been shown that on a decadal timescale there is a statistically significant relationship between oceanographic conditions in west Spitsbergen fjords (Isfjorden) and the combined effect of external factors, such as temperature in the core of the WSC and wind-stress-induced surface Ekman drift to the west of Svalbard. It is important to note that our calculations show that the maximum temperatures in the different layers of the investigated fjord responds differently to external forcing, with a higher correlation to atmospheric forcing in the sub-surface layer and to mean conditions of the WSC in the bottom layer. This implies that interannual changes in large-scale atmospheric circulation in the Arctic and in Fram Strait might be of substantial importance for shelf–fjord water exchange and temperature in west Spitsbergen fjords.

Acknowledgements

Oceanographic data were compiled from the ICES oceanographic database (http://www.ices.dk/datacentre/) and the World Data Centre Oceanographic database, Obninsk, Russia. ERA-40 and ERA-Interim data used in this study have been obtained from the European Centre for Medium-Range Weather Forecasts data server (http://data.ecmwf.int/data). Data on WSC hydrography along the Sørkapp Section were kindly provided by the Institute of Marine Research, Norway. This study was partly funded by the Research Council of Norway through grant no. 196211/S30 (Polar Research Programme). The work was finalized during a research stay of AP at the NPI, funded by the Research Council of Norway's Yggdrasil programme 2010–11 (grant no. 202423/V11). AP thanks the joint AARI–NPI Fram Arctic Climate Research Laboratory for financial support. We thank Stephen Hudson (NPI) for valuable comments and discussion. Constructive comments from reviewers aided in significantly improving this manuscript.

References

Aagaard K. & Greisman P. 1975. Toward new mass and heat budgets for the Arctic Ocean. *Journal of Geophysical Research 80*, 3821–3827.

Andreev O.M. & Ivanov B.V. 2001. Parameterization of radiation processes in the ice-cover model. *Russian Meteorology and Hydrology 2*, 81–88.

Basedow S.L., Eiane K., Tverberg V. & Spindler M. 2004. Advection of zooplankton in an Arctic fjord (Kongsfjord, Svalbard). *Estuarine, Coastal and Shelf Science 60*, 113–124.

Berge J., Johnsen G., Nilsen F., Gulliksen B. & Slagstad D. 2005. Ocean temperature oscillations enable reappearance of blue mussels *Mytilus edulis* in Svalbard after a 1000 year absence. *Marine Ecology Progress Series 303*, 167–175.

Berge J., Renaud P.E., Eiane K., Gulliksen B., Cottier F.R., Varpe O. & Brattegard T. 2009. Changes in the decapod fauna of an Arctic fjord during the last 100 years (1908–2007). *Polar Biology 32*, 953–961.

Bromwich D.H., Fogt R.L., Hodges K.E. & Walsh J.E. 2007. A tropospheric assessment of the ERA-40, NCEP, and JRA-25 global reanalyses in the polar regions. *Journal of Geophysical Research—Atmospheres 112*, D10111, doi: 10.1029/2006JD007859.

Carmack E.C., Macdonald R.W., Perkin R.G., McLaughlin F.A. & Pearson R.J. 1995. Evidence for warming of Atlantic Water in the Southern Canadian Basin of the Arctic Ocean: results from the Larsen-93 Expedition. *Geophysical Research Letters 22*, 1061–1064.

Carton J.A., Chepurin G.A., Reagan J. & Häkkinen S. 2011. Interannual to decadal variability of Atlantic Water in the Nordic and adjacent seas. *Journal of Geophysical Research—Oceans 116*, C11035, doi: 10.1029/2011JC007102.

Coachman L.K. & Aagaard K. 1974. Physical oceanography of the Arctic and sub-Arctic seas. In Y. Herman (ed.): *Marine Geology and Oceanography of the Arctic Ocean*. Pp. 1–72. New York: Springer.

Cottier F.R., Nilsen F., Inall M.E., Gerland S., Tverberg V. & Svendsen H. 2007. Wintertime warming of an Arctic shelf in response to large-scale atmospheric circulation. *Geophysical Research Letters 34*, L10607, doi: 10.1029/2007GL029948.

Cottier F.R., Tverberg V., Inall M.E., Svendsen H., Nilsen F. & Griffiths C. 2005. Water mass modification in an Arctic fjord through cross-shelf exchange. *Journal of Geophysical Research—Oceans 110*, e12005, doi: 10.1029/2004JC002757.

Dee D.P., Uppala S.M., Simmons A.J., Berrisford P., Poli P., Kobayashi S., Andrae U., Balmaseda M.A., Balsamo G., Bauer P., Bechtold P., Beljaars A.C.M., van de Berg L., Bidlot J., Bormann N., Delsol C., Dragani R., Fuentes M., Geer A.J., Haimberger L., Healy S.B., Hersbach H., Hólm E.V., Isaksen L., Kållberg P., Köhler M., Matricardi M., McNally A.P., Monge-Sanz B.M., Morcrette J.-J., Park B.-K., Peubey C., de Rosnay P., Tavolato C., Thépaut J.-N. & Vitart F. 2011. The ERA-Interim reanalysis: configuration and performance of the data assimilation system. *Quarterly Journal of the Royal Meteorological Society 137*, 553–597.

Grotefendt K., Logemann K., Quadfasel D. & Ronski S. 1998. Is the Arctic Ocean warming? *Journal of Geophysical Research—Oceans 103*, 27679–27687.

Hanzlick D.J. 1983. *The West Spitsbergen Current: transport, forcing and variability*. PhD thesis, University of Washington, Seattle.

Hop H., Pearson T., Hegseth E.N., Kovacs K.M., Wiencke C., Kwasniewski S., Eiane K., Mehlum F., Gulliksen B., Wlodarska-Kowalczuk M., Lydersen C., Weslawski J.M., Cochrane S., Gabrielsen G.W., Leakey R.J.G., Lonne O.J., Zajaczkowski M., Falk-Petersen S., Kendall M., Wangberg S.-A., Bischof K., Voronkov A.Y., Kovaltchouk N.A., Wiktor J., Poltermann M., di Prisco G., Papucci C. & Gerland S. 2002. The marine ecosystem of Kongsfjorden, Svalbard. *Polar Research 21*, 167–208.

Ganachaud A. & Wunsch C. 2000. Improved estimates of global ocean circulation, heat transport and mixing from hydrographic data. *Nature 408*, 453–457.

Ingvaldsen R., Reitan M.B., Svendsen H. & Asplin L. 2001. The upper layer circulation in the Kongsfjorden and Krossfjorden—a complex fjord system on the west coast of Spitsbergen. In O. Watanabe & T. Yamanouchi (eds.): *Memoirs of National Institute of Polar Research 54,* Pp. 393–407. Tokyo: National Institute of Polar Research.

Jakobsson M., Macnab R., Mayer L., Anderson R., Edwards M., Hatzky J., Schenke H.W. & Johnson P. 2008. An improved bathymetric portrayal of the Arctic Ocean: implications for ocean modeling and geological, geophysical and oceanographic analyses. *Geophysical Research Letters 35*, L07602, doi: 10.1029/2008gl033520.

Johannessen J.A., Johannessen O.M., Svendsen E., Shuchman R., Manley T., Campbell W.J., Josberger E.G., Sandven S., Gascard J.C., Olaussen T., Davidson K. & Van Leer J. 1987. Mesoscale eddies in the Fram Strait Marginal Ice Zone during the 1983 and 1984 Marginal Ice Zone Experiments. *Journal of Geophysical Research—Oceans 92*, 6754–6772.

Klinck J.M., O'Brien J.J. & Svendsen H. 1981. A simple model of fjord and coastal circulation interaction. *Journal of Physical Oceanography 11*, 1612–1626.

Kwok R. 2009. Outflow of Arctic Ocean sea ice into the Greenland and Barents seas: 1979–2007. *Journal of Climate 22*, 2438–2457.

Lind S. & Ingvaldsen R.B. 2012. Variability and impacts of Atlantic Water entering the Barents Sea from the north. *Deep-Sea Research Part I 62*, 70–88.

Nansen F. 1915. *Spitsbergen waters; oceanographic observations during the cruise of the Veslemöy to Spitsbergen in 1912. Vitenskapsselskapets Skrifter 1. Matematisk–Naturvitenskapelig Klasse*. Kristiania: Videnskapsselskapet.

Nilsen F., Cottier F., Skogseth R. & Mattsson S. 2008. Fjord–shelf exchange controlled by ice and brine production: the interannual variation of Atlantic Water in Isfjorden, Svalbard. *Continental Shelf Research 28*, 1838–1853.

Nilsen F., Gjevik B. & Schauer U. 2006. Cooling of the West Spitsbergen Current: isopycnal diffusion by topographic vorticity waves. *Journal of Geophysical Research—Oceans 11*, C08012, doi: 10.1029/2005JC002991.

Polyakov I.V., Alekseev G.V., Timokhov L.A., Bhatt U.S., Colony R.L., Simmons H.L., Walsh D., Walsh J.E. & Zakharov V.F. 2004. Variability of the intermediate Atlantic water of the Arctic Ocean over the last 100 years. *Journal of Climate 17*, 4485–4497.

Polyakov I.V., Alexeev V.A., Ashik I.M., Bacon S., Beszczynska-Möller A., Carmack E.C., Dmitrenko I.A., Fortier L., Gascard J.-C., Hansen E., Hölemann J., Ivanov V.V., Kikuchi T., Kirillov S., Lenn Y.-D., McLaughlin F., Piechura J., Repina I., Timokhov L.A., Walczowski W. & Woodgate R. 2011. NOWCAST: fate of early-2000s Arctic warm water pulse. *Bulletin of American Meteorological Society 92*, 561–565.

Rudels B., Meyer R., Fahrbach V., Ivanov V.V., Østerhus S., Quadfasel D., Schauer U., Tverberg V. & Woodgate R.A. 2000. Water mass distribution in Fram Strait and over the Yermak Plateau in summer 1997. *Annales Geophysicae 18*, 687–705.

Saloranta T.M. & Haugan P.M. 2001. Interannual variability in the hydrography of Atlantic Water northwest of Svalbard. *Journal of Geophysical Research—Oceans 106*, 13931–13943.

Saloranta T.M. & Haugan P.M. 2004. Northward cooling and freshening of the warm core of the West Spitsbergen Current. *Polar Research 23*, 79–88.

Saloranta T.M. & Svendsen H. 2001. Across the Arctic Front west of Spitsbergen: high-resolution CTD sections from 1998–2000. *Polar Research 20*, 177–184.

Schauer U., Beszczynska-Moller A., Walczowski W., Fahrbach E., Piechura J. & Hansen E. 2008. Variation of measured heat flow through the Fram Strait Between 1997 and 2006. In R. R. Dickson et al. (eds.): *Arctic–Subarctic ocean fluxes: defining the role of the northern seas in climate*. Pp. 65–85. Dordrecht: Springer.

Schroeder L.D., Sjoquist D.L. & Stephan P.E. 1986. *Understanding regression analysis: an introductory guide*. Newbury Park, CA: SAGE.

Smedsrud L.H., Ingvaldsen R., Nilsen J.E.O. & Skagseth O. 2010. Heat in the Barents Sea: transport, storage, and surface fluxes. *Ocean Science 6*, 219–234.

Spielhagen R.F., Werner K., Sorensen S.A., Zamelczyk K., Kandiano E., Budeus G., Husum K., Marchitto T.M. & Hald M. 2011. Enhanced modern heat transfer to the Arctic by warm Atlantic Water. *Science 331*, 450–453.

Svendsen H., Beszczynska-Moller A., Hagen J.O., Lefauconnier B., Tverberg V., Gerland S., Orbaek J.B., Bischof K., Papucci C., Zajaczkowski M., Azzolini R., Bruland O., Wiencke C., Winther J.-G. & Dallmann W. 2002. The physical environment of Kongsfjorden–Krossfjorden, an Arctic fjord system in Svalbard. *Polar Research 21*, 133–166.

Teigen S.H., Nilsen F. & Gjevik B. 2010. Barotropic instability in the West Spitsbergen Current. *Journal of Geophysical Research—Oceans 115*, C07016, doi: 10.1029/2009JC005996.

Teigen S.H., Nilsen F., Skogseth R., Gjevik B. & Beszczynska-Möller A. 2011. Baroclinic instability in the West Spitsbergen Current. *Journal of Geophysical Research—Oceans 116*, C07012, doi: 10.1029/2011JC006974.

Treshnikov A.F. 1977. Water masses of the Arctic Basin. In M.J. Dunbar (ed.): *Proceedings of the Polar Oceans Conference*. Pp. 17–31. Calgary: Arctic Institute of North America.

Trešnikov [Treshnikov] A.F. & Baranov G.I. 1972. *Struktura cirkuljacii vod Arktičeskogo bassejna. (The structure of Arctic Water circulation.)* Leningrad: Gidrometeoizdat.

Tverberg V., Nilsen F., Goszczko I., Cottier F., Svendsen H. & Gerland S. 2007. The warm winter temperatures of 2006 and 2007 in the Kongsfjorden water masses compared to historical data. In R. Azzolini (ed.): *8th Ny-Alesund seminar. Polarnet technical report*. Pp. 40–44. Rome: Earth and Environment Department, National Research Council.

Tverberg V. & Nøst O.A. 2009. Eddy overturning across a shelf edge front: Kongsfjorden, west Spitsbergen. *Journal of Geophysical Research—Oceans 114*, C04024, doi: 10.1029/2008JC005106.

Vinje T. 2001. Fram Strait ice fluxes and atmospheric circulation: 1950–2000. *Journal of Climate 14*, 3508–3517.

Walczowski W. & Piechura J. 2007. Pathways of Greenland Sea warming. *Geophysical Research Letters 34*, L10608, doi: 10.1029/2007GL029974.

Zhuravskiy D., Ivanov B. & Pavlov A. 2012. Ice conditions at Gronfjorden Bay, Svalbard, from 1974 to 2008. *Polar Geography 35*, 169–176.

Citation: *Polar Research* 2013, *32*, 11206, http://dx.doi.org/10.3402/polar.v32i0.11206